

ORIGINAL ARTICLE

Functional impact of NOTCH1 mutations in chronic lymphocytic leukemia

F Arruga¹, B Gizdic^{1,2}, S Serra^{1,3}, T Vaisitti¹, C Ciardullo⁴, M Coscia⁵, L Laurenti⁶, G D'Arena⁷, O Jaksic², G Inghirami⁸, D Rossi⁴, G Gaidano⁴ and S Deaglio^{1,3}

The purpose of this study was to compare the expression and function of NOTCH1 in chronic lymphocytic leukemia (CLL) patients harboring a wild-type (WT) or mutated *NOTCH1* gene. *NOTCH1* mRNA and surface protein expression levels were independent of the *NOTCH1* gene mutational status, consistent with the requirement for NOTCH1 signaling in this leukemia. However, compared with *NOTCH1*-WT CLL, mutated cases displayed biochemical and transcriptional evidence of an intense activation of the NOTCH1 pathway. *In vivo*, expression and activation of NOTCH1 was highest in CLL cells from the lymph nodes as confirmed by immunohistochemistry. *In vitro*, the NOTCH1 pathway was rapidly downregulated, suggesting that signaling relies upon micro-environmental interactions even in *NOTCH1*-mutated cases. Accordingly, co-culture of Jagged1⁺ (the NOTCH1 ligand) nurse-like cells with autologous CLL cells sustained NOTCH1 activity over time and mediated CLL survival and resistance against pro-apoptotic stimuli, both abrogated when NOTCH1 signaling was pharmacologically switched off. Together, these results show that *NOTCH1* mutations have stabilizing effects on the NOTCH1 pathway in CLL. Furthermore, micro-environmental interactions appear critical in activating the NOTCH1 pathway both in WT and mutated patients. Finally, NOTCH1 signals may create conditions that favor drug resistance, thus making NOTCH1 a potential molecular target in CLL.

Leukemia (2014) 28, 1060–1070; doi:10.1038/leu.2013.319

Keywords: chronic lymphocytic leukemia; *NOTCH1* mutations; micro-environment

INTRODUCTION

Chronic lymphocytic leukemia (CLL), one of the most common types of adult leukemia in Western countries, is characterized by the accumulation of mature CD5⁺/CD23⁺ B lymphocytes in the peripheral blood (PB) and lymphoid organs.¹ Mainly diagnosed in older adults, CLL is heterogeneous in terms of progression, therapeutic response and outcome. Research to identify prognostic biological markers for CLL has therefore been a major priority and has yielded fruitful results.^{2–7} Recently, next-generation sequencing of the CLL exome has revealed previously unrecognized genetic lesions.^{8–12} Among these, *NOTCH1* mutations characterize 5–10% of newly diagnosed CLL cases, with their prevalence increasing to 15–20% in progressive or relapsed patients.¹³ *NOTCH1* mutations are found preferably in CLL with unmutated immunoglobulin heavy variable (*IGHV*) genes and even more frequently in CLL that harbor trisomy 12, where they identify a distinct clinico-molecular subgroup characterized by deregulated cell cycle and short survival.^{14,15}

NOTCH1 encodes a transmembrane receptor acting as a ligand-activated transcription factor.^{16,17} NOTCH1 signaling initiates when the ligand, from either the Jagged or Delta families, binds to the receptor and induces successive proteolytic cleavages, resulting in the release and nuclear translocation of the NOTCH1 intra-cellular domain (NICD). In the nucleus, the NICD assembles a transcriptional complex that interacts with the transcription factor

CBF1/RBP-Jk, leading to de-repression/activation of CBF1-dependent target genes.^{18–20} Several members of the hairy/enhancer of split (Hes) family of the basic helix–loop–helix proteins including *HES1* are direct NOTCH1/CBF1 transcriptional targets.^{21,22} Besides this canonical pathway, NOTCH1 also activates *Deltex1* (*DTX1*), which binds to the ankyrin repeats of the NICD, likely antagonizing CBF1 binding.^{23,24} In mammalian cells, *DTX1* has been shown to be a transcriptional target of NOTCH1 itself, suggesting a positive feedback loop between NOTCH1 and *DTX1*. Furthermore, *DTX1* may bind to the nuclear coactivator EP300, perturbing EP300 interactions with the transcription factor TCF3/E2A.^{25,26} A role for this non-canonical NOTCH1 pathway in tumor transformation has recently been proposed.²⁷

NOTCH1 is constitutively expressed by CLL cells, where it increases cell survival and induces apoptosis resistance.^{28,29} Moreover, leukemic cells express *JAG1*/Jagged1 and *JAG2*/Jagged2 ligands, suggesting autocrine/paracrine loops for NOTCH1 signaling activation.²⁸

NOTCH1 mutations in CLL cluster in exon 34 are selected to disrupt the C-terminal PEST domain of the protein, responsible for the proteosomal degradation of the activated form of NOTCH1, and associate with a specific gene expression signature, suggesting a major impact on the biology of mutated cells.^{8,13} Even if truncation of the PEST domain by *NOTCH1* mutations is predicted to result in NOTCH1-impaired degradation, stabilization of the

¹Department of Medical Sciences, University of Turin, School of Medicine, Turin, Italy; ²Department of Hematology, Dubrava University Hospital, Zagreb, Croatia; ³Human Genetics Foundation (HuGeF), Turin, Italy; ⁴Division of Hematology, Department of Translational Medicine, Amedeo Avogadro University of Eastern Piedmont, Novara, Italy; ⁵Division of Hematology, Laboratory of Hematology Oncology, Center of Experimental Research and Medical Studies, Città della Salute e della Scienza University Hospital, Turin, Italy; ⁶Institute of Hematology, Catholic University of the Sacred Heart, Rome, Italy; ⁷Department of Onco-Hematology, IRCCS Centro di Riferimento Oncologico della Basilicata, Rionero in Vulture, Italy and ⁸Department of Molecular Biotechnology and Health Sciences, Center of Experimental Research and Medical Studies, University of Turin, Turin, Italy. Correspondence: Dr S Deaglio, Department of Medical Sciences, University of Turin, School of Medicine and Human Genetics Foundation (HuGeF), via Nizza, 52, 10126 Turin, Italy. E-mail: silvia.deaglio@unito.it

Received 21 October 2013; accepted 24 October 2013; accepted article preview online 30 October 2013; advance online publication, 19 November 2013

active form of the molecule and deregulated signaling,³⁰ a formal demonstration of the functional effects of *NOTCH1* mutations in CLL cells is still lacking. On these bases, the present study was undertaken to compare the expression and functional role of NOTCH1 in wild-type (WT) or mutated CLL patients.

PATIENTS AND METHODS

Patient samples and cell lines

Biological samples were obtained after informed consent, in accordance with Institutional Guidelines and Declaration of Helsinki. Patients' characteristics are reported in Supplementary Materials and Methods (SMM) and Supplementary Table 1. PB mononuclear cells (PBMCs) and purified B lymphocytes were prepared as described in SMM.

Paired PB, bone marrow (BM) and lymph node (LN) samples from the same patient were made available by the Department of Hematology of Dubrava University Hospital (Supplementary Table 2).

Nurse-like cells (NLC) were generated as described.³¹

MEC-1 (CLL-like), Molt-4/IG (T-ALL clone of Molt-4) and Nalm-6 (pre-B-ALL) were cultured in RPMI-1640 medium with 10% heat-inactivated fetal calf serum and penicillin streptomycin (100 IU/ml, all obtained from Sigma, Milan, Italy).

NOTCH1 mutational analysis

NOTCH1 mutational status was determined as reported.¹³ Sanger-based sequencing analysis of exon 34 was performed for each patient. The percentage of mutant alleles was determined using a Custom TaqMan SNP Genotyping Assay (Applied Biosystems, Life Technologies, Monza, Italy), see SMM.

Reagents

Gamma-secretase inhibitor (GSI)IX was obtained from Merck (Darmstadt, Germany), Marimastat (matrix metalloprotease inhibitor) was obtained from Tocris (Bristol, UK) and fludarabine (2-Fluoroadenine-9- β -D-arabinofuranoside) was obtained from Sigma-Aldrich (Milan, Italy).

CLL-NLC co-cultures

Two different CLL-NLC co-culture approaches were used. In the first, CLL lymphocytes remaining viable after the NLC differentiation process were gently collected and analyzed. In the second, CLL lymphocytes remaining viable after the NLC differentiation process were removed. Autologous purified CLL lymphocytes, frozen at the time of sample arrival, were thawed and added to the culture (0.5×10^6 for each 48 well) for the indicated time points.

Flow cytometry

Antibodies used for flow cytometry were anti-CD5-FITC, -CD19-PE, -NOTCH1-APC (eBiosciences, Milan, Italy), anti-CD19-PerCP (Aczon, Bologna, Italy), anti-Jagged1 (from Vinci-Biochem, Florence, Italy) and anti-Jagged2-PE, -DLL1-PE, -DLL4-PE (from Biolegend, Milan Italy).

Data were acquired using a FACSCanto II cytofluorimeter (BD Biosciences, Milan, Italy) and processed with DIVA v6.1.3 and FlowJo Version 9.01 (TreeStar, Ashland, OR, USA).

RNA extraction and quantitative real-time PCR

RNA was extracted using the RNeasy Plus Mini Kit (Qiagen, Milan Italy) and retro-transcribed using the Reverse Transcription Kit (Applied Biosystems). Quantitative real-time PCR (qRT-PCR) was conducted with the 7900 HT Fast Real-Time PCR System (SDS2.3 software, Applied Biosystems). Primers and analysis of the results are detailed in SMM.

Western blot

Cells were lysed as described.³² Proteins were resolved by SDS-PAGE or by Nu-PAGE 3–8% Tris-Acetate gel (Life Technologies) and transferred to nitrocellulose membranes (Life Sciences, Bio-Rad, Segrate, Italy). Antibodies used were: anti-total NOTCH1 (Abcam, Cambridge, UK; clone no. 27526), anti-cleaved NOTCH1 and anti-HES1 (both from Cell Signaling Technology, Pero, Italy; clone no. D3B8 and clone D6P2U) and anti-ERK1/2 (BD Transduction Laboratories, clone no. 610124). Image acquisition and densitometric analyses were performed using ImageQuant LAS4000 and

TL Version 7.0 software (GE Healthcare, Milan, Italy). Band intensities were calculated by standardizing over total ERK1/2 expression levels. The Molt-4/IG cell line was used as an internal loading control in the different gels.

Immunohistochemistry and immunofluorescence

LN sections were obtained from the Department of Molecular Biotechnology and Health Sciences of the University of Turin, the Department of Pathology of the University of Eastern Piedmont (Novara, Italy) and the Department of Hematology of Dubrava University (Zagreb, Croatia). Formalin-fixed, paraffin-embedded sections from 22 LN samples were deparaffinized and endogenous peroxidase activity was blocked. Epitope retrieval was performed in 0.01 M citrate buffer, pH 6.0 (40 m, 98 °C). Antibodies used for immunohistochemistry or immunofluorescence studies were: rabbit polyclonal anti-NOTCH1 (Abcam, clone no. 27526, which binds a peptide at the C terminus, before the c.7544_7545delCT mutation), rabbit monoclonal anti-Jagged1 (Abcam, clone no. EPR4290), mouse monoclonal anti-CD68 (Abcam, clone no. KP1) and goat polyclonal anti-CD23/Fc (R&D Systems, Minneapolis, MN, USA). Anti-rabbit horse radish peroxidase-conjugated Abs and 3,3'-diaminobenzidine (EnVision System, Dako, Milan, Italy) were used to visualize the reaction.

For immunofluorescence, tissue sections or glass coverslips were incubated with the following secondary Abs: AlexaFluor 633-conjugated goat anti-mouse IgG (1:250; Invitrogen, Milan, Italy), DyLight 488-conjugated bovine anti-goat IgG and DyLight 594-conjugated donkey anti-rabbit IgG (1:300, both obtained from Jackson ImmunoResearch, West Grove, PA, USA). Alexa-568-conjugated phalloidin (Life Technologies) and DAPI (4,6 diamidino-2-phenylindole) were used to counterstain.

Slides were analyzed using a DMI 3000 B optical microscope (Leica Microsystems, Milan, Italy), equipped with a DCF 310 FX digital camera and LAS Version 3.8 software. For immunofluorescence experiments, slides were mounted in SlowFade Gold reagent (Invitrogen) and analyzed using a TCS SP5 laser scanning confocal microscope with four lasers (Leica Microsystems). Images were acquired with the LAS AF software (version Lite 2.4) and processed with Adobe Photoshop (Adobe Systems, San Jose, CA, USA). Pixel intensity and raw integrated density analyses were performed using ImageJ (<http://rsbweb.nih.gov/ij/>).

Apoptosis assay

Apoptosis was measured using the Annexin-V FITC Apoptosis Kit (Invitrogen).

Detection of soluble jagged1 and -2

Soluble Jagged1 and Jagged2 were quantified using enzyme-linked immunosorbent assay kits (Antibodies-online GmbH, Germany).

Statistical analysis of data

Statistical analyses were performed with GraphPad version 5 (GraphPad Software Inc., La Jolla, CA, USA) and are detailed in SMM.

RESULTS

Expression of NOTCH1 and its ligands in mutated and WT CLL patients

The first step of this study was the analysis of the expression of NOTCH1 and its ligands by CLL cells. The cohort included 21 *NOTCH1*-mutated and 21 WT patients, all expressing unmutated *IGHV* genes. The *NOTCH1*-mutated subset was enriched in patients with trisomy 12 (9/19, 43% in the mutated vs 1/18, 6% in the WT subset, Supplementary Table 1), as expected.^{14,15}

CLL lymphocytes expressed *NOTCH1* mRNA at high levels, without measurable differences between *NOTCH1*-mutated or WT patients (Figure 1a). This finding confirms previous data showing that expression in CLL samples is relatively homogeneous.²⁸

In line with these results, NOTCH1 protein was expressed by the majority of CD19⁺/CD5⁺ CLL cells, with no differences between the two subsets, either in terms of percentage of positive cells or of mean fluorescence intensity (MFI; Figure 1b).

CLL cells expressed *JAG1* and *JAG2* transcripts (Figure 1c and Supplementary Figure 1), whereas they lacked DLL1 or DLL4 (not shown). No differences were detected between *NOTCH1*-mutated

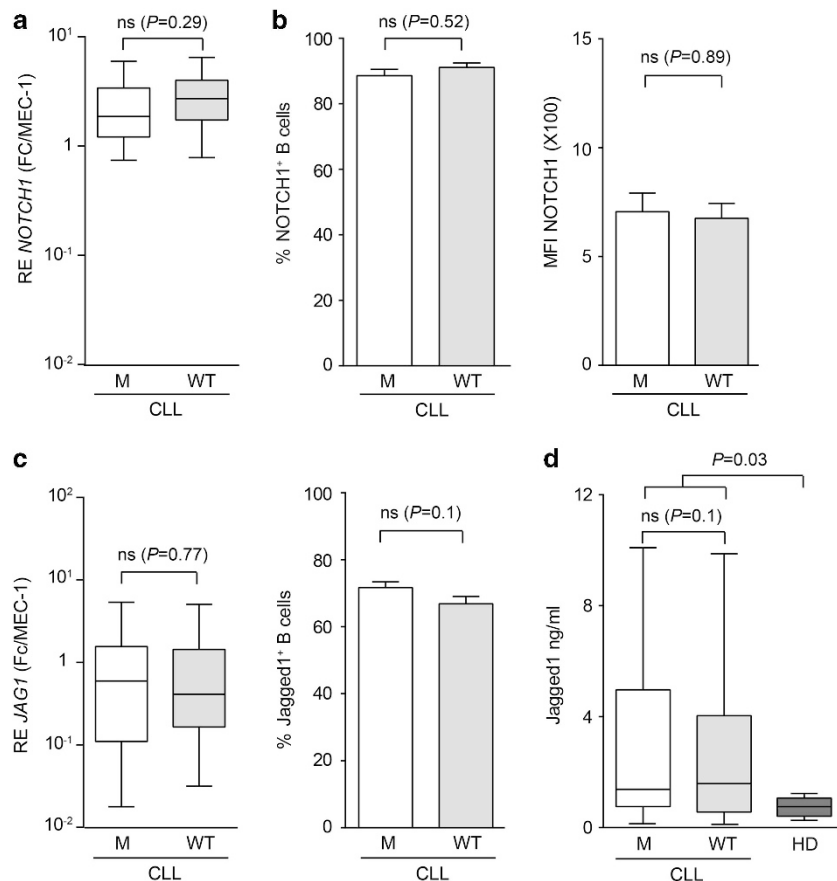


Figure 1. Expression of NOTCH1 and Jagged1 in CLL cells from NOTCH1-mutated and WT patients. **(a)** Box plot representing qRT-PCR data of NOTCH1 mRNA levels in B lymphocytes purified from CLL patients classified according to the presence (M, $n = 21$) or absence (WT, $n = 21$) of NOTCH1 mutations. NOTCH1 mRNA levels were normalized on β -actin mRNA as housekeeping gene. Mean $\Delta\Delta CT$ in NOTCH1-mutated patients was 2.78 ± 0.39 vs 3.31 ± 0.38 in WT patients. Relative expression is the result of normalization of CLL values over those of MEC-1, added for calibration purposes. **(b)** Percentage (left) and MFI (right) of NOTCH1⁺ cells in CD19⁺/CD5⁺ CLL lymphocytes, divided according to the presence (M, $n = 21$) or absence (WT, $n = 21$) of NOTCH1 mutations. Mean % of NOTCH1⁺ cells 88.56 ± 1.96 in the mutated vs 91.09 ± 1.36 in the WT subgroup; mean MFI values in mutated 706 ± 85.53 vs 675.9 ± 68.42 in WT patients. Data are expressed as mean \pm s.e.m. **(c)** (Left) qRT-PCR data showing relative expression of JAG1 in B lymphocytes purified from CLL patients classified according to the presence (M, $n = 21$) or absence (WT, $n = 21$) of NOTCH1 mutations. Mean $\Delta\Delta CT$ of JAG1 1.1 ± 0.34 in mutated vs 1.0 ± 0.28 in WT patients. (Right) Histograms representing the percentage of Jagged1⁺ B lymphocytes from CLL patients categorized according to the presence (M, $n = 21$) or absence (WT, $n = 21$) of NOTCH1 mutations. Mean % of CD19⁺/CD5⁺/Jagged1⁺ in mutated 71.71 ± 7.736 vs 66.86 ± 9.787 in WT CLL patients. Data are expressed as mean \pm s.e.m. **(d)** Box plot showing the results of an enzyme-linked immunosorbent assay performed on plasma from CLL patients (M, $n = 21$; WT, $n = 62$) or normal individuals (HD, $n = 8$) to quantify soluble Jagged1. Mean ng/ml in plasma of mutated 2.93 ± 1.44 vs 2.77 ± 2.04 in WT patients vs 0.73 ± 0.12 in plasma from age- and sex-matched controls.

or WT patients. At the protein level, CLL lymphocytes stained homogeneously positive for Jagged1 and Jagged2, either in terms of percentage of positive cells or of MFI (Figure 1c and Supplementary Figure 1).

The plasma of CLL patients contained Jagged1 in significantly higher amounts than the plasma obtained from age- and sex-matched healthy donors ($P = 0.03$, Figure 1d). Low levels of Jagged2 were also detected in the plasma of CLL patients and of normal donors (Supplementary Figure 1).

Activation of NOTCH1 pathway in mutated and WT patients

Next, constitutive activation of NOTCH1 pathway in circulating CLL lymphocytes was studied by gene profiling and biochemical approaches. Expression of *HES1* and *DTX1* was selected as hallmark of activation of the canonical and non-canonical NOTCH1 pathways, respectively. Both genes were significantly upregulated in NOTCH1-mutated CLL compared with WT cases ($P = 0.02$ for *HES1*, Figure 2a; $P = 0.03$ for *DTX1*, Figure 2b).

Differential activation of the NOTCH1 pathway in the two patient subsets was confirmed using biochemical assays. An antibody recognizing total NOTCH1 and one specific for the NICD were used to detect distinct molecular species. Experimental conditions were set up using Molt-4/IG (T-ALL, NOTCH1⁺, activating mutation in the heterodimerization domain but WT in the PEST domain), Nalm-6 (pre-B-ALL and NOTCH1⁺) and MEC-1 (CLL-like, NOTCH1⁺ and WT). The antibody recognizing total NOTCH1 highlighted a band in Molt-4/IG and MEC-1 lysates of ~ 110 kDa, compatible with the transmembrane form and a higher band of ~ 300 kDa, compatible with the precursor protein (Supplementary Figure 2). No specific band could be highlighted in the Nalm-6 lysate. A prominent band corresponding to the NICD was apparent in the Molt-4/IG lysate, in line with the presence of a constitutively activated pathway (Supplementary Figure 2). Pretreatment of Molt-4/IG cells with GSIX, a gamma-secretase inhibitor, induced a dose-dependent loss of the band corresponding to NICD and of the *Hes1* target (Figure 2c). A sharp decrease in the transcription of *HES1* and *DTX1* was also observed, confirming

that GSiIX can be used to inhibit the NOTCH1 pathway (Figure 2d). GSiIX treatment also induced a dose-dependent accumulation of a second band, compatible with NEXT, a molecular intermediate of the transmembrane form, cleaved by the metalloproteases but not by the gamma-secretase complex (Figure 2e).³³ The use of Marimastat, a metalloprotease inhibitor, in combination with GSiIX

prevented accumulation of NEXT in a dose-dependent way (Figure 2e).

A panel of *NOTCH1*-mutated and WT patients was then analyzed using the same antibody grid. The patients selected for analysis carried a comparable load of *NOTCH1* mutations (Supplementary Table 2). WT patients showed a major band at ~110 kDa, compatible with the transmembrane form highlighted in Molt-4/IG and MEC-1 cells. Mutated patients invariably displayed a second band of slightly lower molecular weight, compatible with NEXT, suggesting marked differences in global NOTCH1 processing in mutated patients (Figure 2f). With this antibody, the mutant allele could not be highlighted. In contrast, when probed with the NICD-specific antibody, *NOTCH1*-mutated patients selectively displayed a prominent band ~10 kDa lower than that of Molt-4/IG (Figure 2f, lower black arrow), which was otherwise absent in *NOTCH1*-WT cases, and, therefore, compatible with the product of the mutant allele. The band corresponding to the WT NICD was less prominent and did not significantly differ in intensity when compared with WT patients (Figure 2f, upper black arrow).

The conclusion of this first part of the work is that circulating CLL cells from *NOTCH1*-mutated cases display evidence of constitutive NOTCH1 pathway activation, despite comparable levels of receptor expression. Furthermore, they show marked differences in the processing of the mutant and the WT *NOTCH1* alleles.

The NOTCH1 pathway is rapidly inactivated following *in vitro* culture of CLL cells

The aim of the second part of the work was to determine how the NOTCH1 pathway is regulated. *NOTCH1*-mutated CLL cells cultured for 24 h showed a sharp decrease of the band corresponding to NICD ($P=0.003$; Figure 3a), reaching the levels of WT patients. A concomitant decrease in *HES1* and *DTX1* levels was highlighted by qRT-PCR ($P=0.008$ for both genes, Figure 3b). *Presenilin1* (*PSEN1*), the main catalytic subunit of the gamma-secretase complex, showed a similar behavior, with decreased expression after culture ($P=0.01$, Figure 3b). This finding offers a partial mechanistic explanation of pathway inhibition.

Inactivation of the pathway, however, was not due to decreased *NOTCH1* expression, as inferred by comparable mRNA levels before and after culture (Figure 3c). At the protein level, NOTCH1 showed a robust increase at the cell surface in mutated patients ($P=0.03$), whereas in WT patients, no differences could be detected

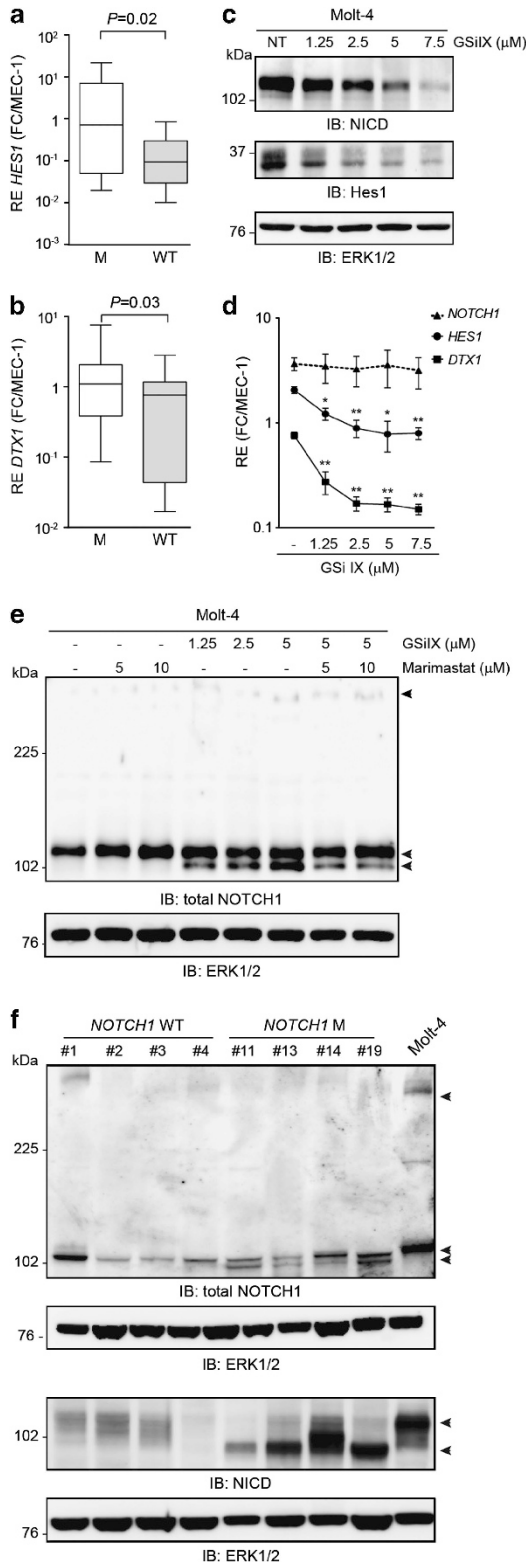
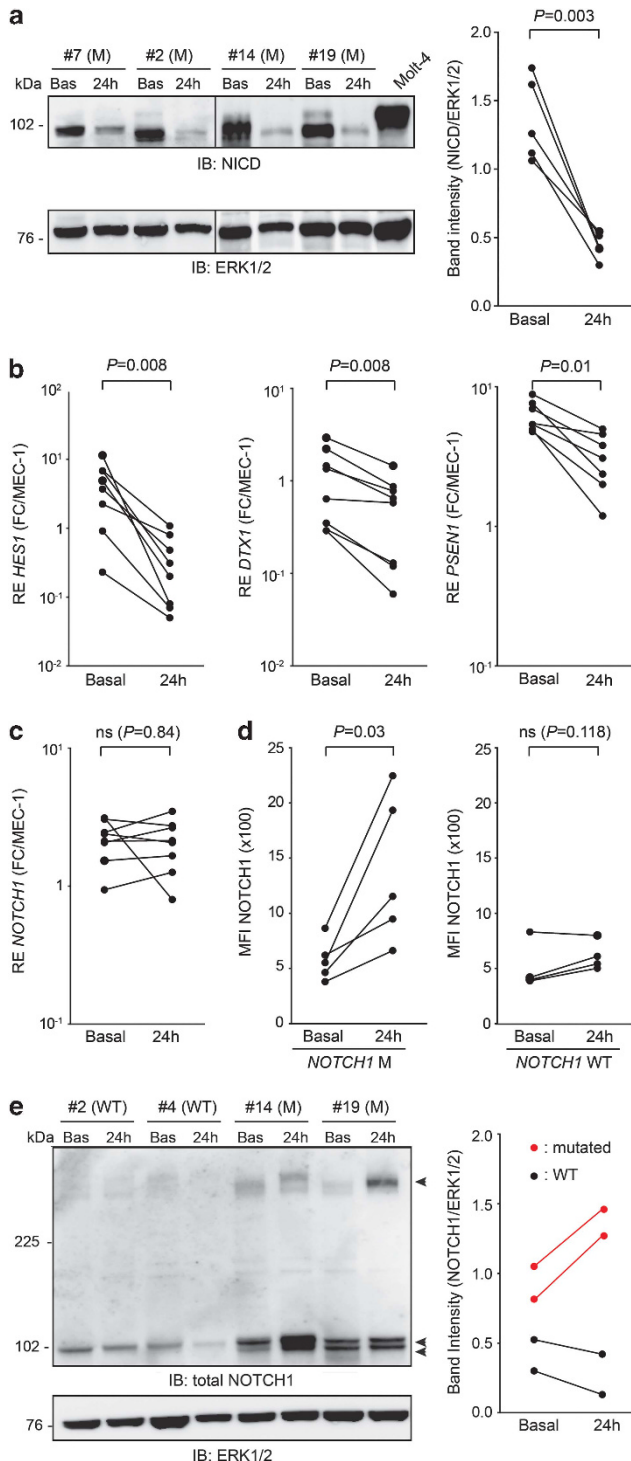


Figure 2. Characterization of NOTCH1 pathway activation in CLL cells from *NOTCH1*-mutated and WT patients. Box plots reporting qRT-PCR data of the expression of *HES1* (a) or *DTX1* (b) in a cohort of CLL patients divided according to *NOTCH1* mutational status ($M=21$, $WT=21$). Mean values of *HES1* 4.41 ± 1.54 in mutated vs 0.24 ± 0.07 in WT patients; mean values of *DTX1* 1.75 ± 0.43 in the mutated vs 0.77 ± 0.18 in the WT subgroup. Relative expression is the result of normalization of CLL values over those of MEC-1, added for calibration purposes. (c) Dose-dependent effects of treatment with GSiIX, a γ -secretase inhibitor, on the expression of NICD (upper panel) and HES1 (middle panel) in the Molt-4/IG cell line. ERK1/2 (lower panel) was used as internal loading control. (d) qRT-PCR data showing *NOTCH1*, *HES1* and *DTX1* expression after GSiIX treatment. Graphs show results of three independent experiments. '*' denotes $P<0.05$, whereas '**' denotes $P<0.005$. (e) Combined effects of GSiIX and Marimastat on total NOTCH1 protein expression in the Molt-4/IG cell line. ERK1/2 was used as internal loading control. Black arrows show distinct NOTCH1 molecular species. (f) Western blot analysis of total NOTCH1 (upper panels) or NICD (lower panels) in four *NOTCH1*-WT and four *NOTCH1*-mutated CLL patients. ERK1/2 was used as internal loading control. Black arrows show distinct NOTCH1 molecular species.

(Figure 3d). These findings suggest an impairment in the generation of NICD in the absence of the ligand, specific for the mutated subset, resulting in accumulation of the molecular species upstream of the proteolytic cut operated by the gamma-secretase complex. This hypothesis was indirectly confirmed by western blot analyses showing increased levels of the precursor, transmembrane and NEXT forms specifically in the mutated subset (Figure 3e).



Differential *in vivo* expression and activation of NOTCH1

These findings suggest that NOTCH1 activation is dependent on conditions selectively active *in vivo*. To measure NOTCH1 expression and activation in different disease compartments, we took advantage of a unique collection of PB, BM and LN samples taken from the same patient at the same time ($n=10$, with two mutated samples indicated in red in the figure, Supplementary Table 3). The percentage of CD19⁺/CD5⁺ cells did not vary significantly in the three compartments and was invariably >80%. *NOTCH1* mRNA levels were significantly higher in the LN as compared with PB and BM ($P=0.01$ and $P=0.006$, respectively; Figure 4a). The same holds true for percentage of expression and MFI (Figure 4b). Western blot analysis of the available samples ($n=3$, no. 1 is shown) confirmed a selective increased in total NOTCH1 in the LN (Figure 4g). Jagged1, on the contrary, showed no measurable differences in the three compartments, whether at the mRNA or protein levels (Figure 4d).

HES1 levels did not differ in the compartments studied (Figure 4e). However, a significant increase in *DTX1* in the LN was evident ($P=0.002$ and $P=0.004$ as compared with PB and BM, respectively; Figure 4e), suggesting that the NOTCH1 non-canonical pathway is selectively activated. Immunohistochemical analyses of LN biopsies ($n=22$) confirmed diffuse NOTCH1 expression by leukemic cells in the LN. Mutated patients ($n=6$) showed preferential nuclear localization of the molecule, whereas localization in WT patients was mostly cytoplasmic ($n=16$; Figure 5a). Jagged1 expression was then checked to infer which cells can trigger NOTCH1 activation *in vivo*. The results show a preferential association of Jagged1 with the stromal architecture surrounding leukemic lymphocytes (Figure 5a). This was confirmed using tissue immunofluorescence that highlighted a colocalization of Jagged1 and CD68, a common marker for stromal cells of myeloid origin (Figures 5b and c).

These results suggest that in the LN, CLL lymphocytes are NOTCH1⁺, whereas the myeloid compartment is Jagged1⁺, supporting the view that the cross talk between CLL lymphocytes and myeloid elements keeps the NOTCH1 pathway active.

Figure 3. Expression and activation of NOTCH1 after *in vitro* culture. (a) (Left) Western blot analysis of NICD on total cell lysates from purified CLL lymphocytes of four *NOTCH1*-mutated patients at baseline and after 24 h *in vitro* cultures. The Molt-4/IG cell line was used as positive control, whereas ERK1/2 as internal loading control. (Right) Graphs representing cumulative data of band intensity quantification from five independent mutated patients. Mean intensity of NICD in basal conditions 1.36 ± 0.13 vs 0.44 ± 0.04 after 24 h cultures. (b) qRT-PCR evaluation of mRNA levels of *HES1*, *DTX1* and *PSEN1* at baseline and after 24 h *in vitro* cultures of purified CLL lymphocytes from eight *NOTCH1*-mutated patients. Mean $\Delta\Delta CT$ of *HES1* in basal conditions 4.62 ± 1.3 vs 0.38 ± 0.13 after 24 h cultures; mean $\Delta\Delta CT$ of *DTX1* in basal conditions 1.2 ± 0.35 vs 0.58 ± 0.17 after 24 h cultures; mean $\Delta\Delta CT$ of *PSEN1* in basal conditions 6.28 ± 0.58 vs 3.14 ± 0.52 after 24 h cultures. Relative expression is the result of normalization of CLL values over those of MEC-1, added for calibration purposes. (c) qRT-PCR analysis of *NOTCH1* mRNA levels in purified CLL lymphocytes at baseline and after 24 h cultures ($n=8$). Mean $\Delta\Delta CT$ of *NOTCH1* in basal conditions 2.2 ± 0.26 vs 2.1 ± 0.3 after 24 h cultures. (d) MFI values of *NOTCH1* expression in basal conditions and after 24 h cultures in *NOTCH1*-mutated ($n=5$, left panel) or WT ($n=4$, right panel) CD19⁺/CD5⁺ CLL cells. Mean MFI in mutated in basal conditions 575.8 ± 82.7 vs 1389 ± 301 after 24 h culture; mean MFI in WT in basal conditions 513 ± 170.3 vs 618 ± 65.9 after 24 h culture. (e) (Left) Western blot analysis of total NOTCH1 protein levels at the baseline and after *in vitro* culture in *NOTCH1*-WT and -mutated patients. ERK1/2 was used as internal loading control. (Right) Band intensities were quantified and normalized over ERK1/2 values. *NOTCH1*-mutated patients are indicated in red.

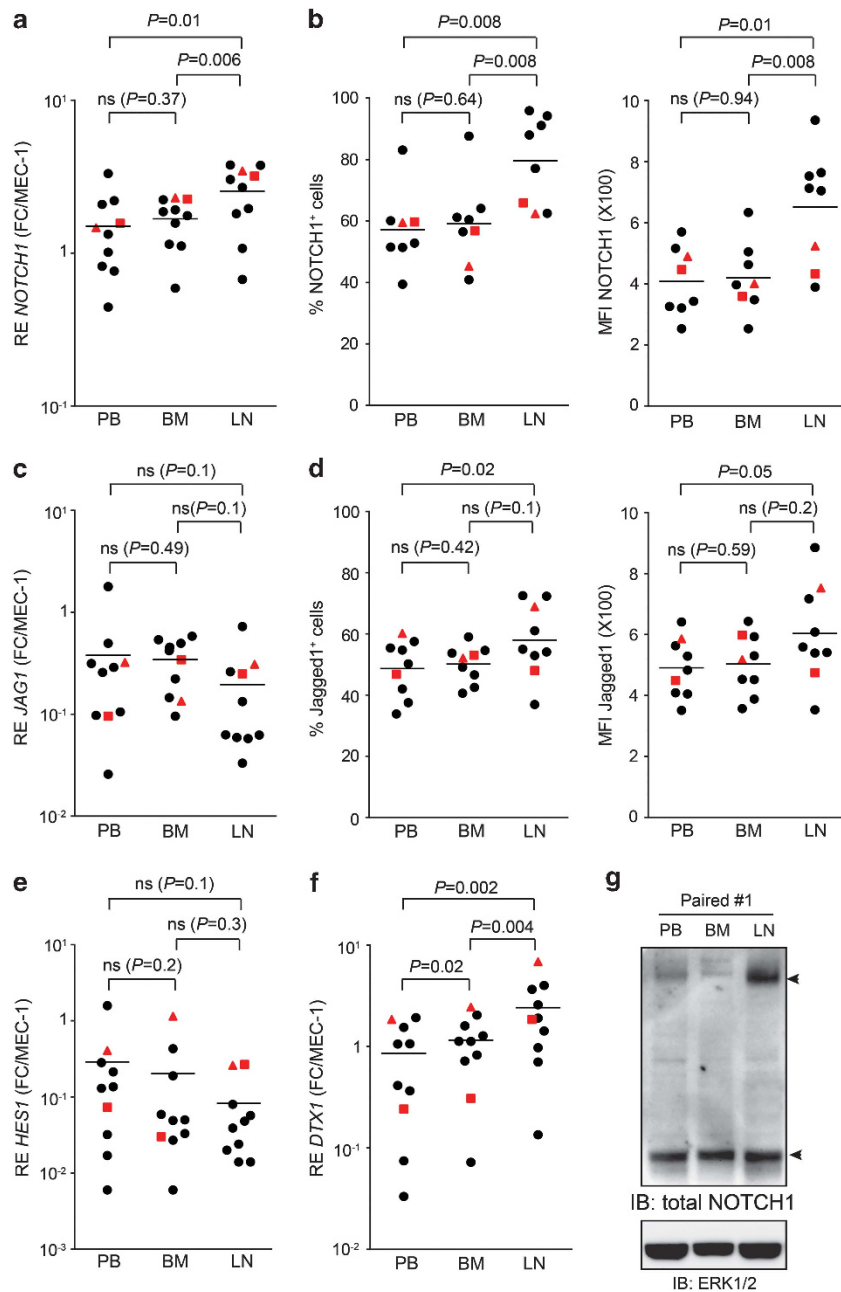


Figure 4. NOTCH1 expression and pathway activation in different disease compartments. (a) qRT-PCR analysis of *NOTCH1* mRNA levels in PB, BM and LN samples obtained from 10 different patients at the same time. Mean $\Delta\Delta CT$ of *NOTCH1* in PB 1.5 ± 0.27 vs 1.67 ± 0.18 in BM vs 2.54 ± 0.35 in LN. Relative expression is the result of normalization of CLL values over those of MEC-1, added for calibration purposes. (b) Percentage (left) and MFI (right) of NOTCH1⁺ cells in CD19⁺/CD5⁺ CLL lymphocytes obtained from paired PB, BM and LN samples. Mean % of CD19⁺/CD5⁺/NOTCH1⁺ cells in PB 57.19 ± 4.4 vs 59.1 ± 4.9 in BM vs 79.6 ± 5.1 in LN; mean MFI in PB 408.3 ± 39.8 vs 420 ± 40.6 in BM vs 652.1 ± 65.9 in LN. (c) qRT-PCR evaluation of *JAG1* mRNA levels in PB, BM and LN paired samples. Mean $\Delta\Delta CT$ 0.38 ± 0.16 in PB vs 0.34 ± 0.06 in BM vs 0.19 ± 0.06 in LN. (d) Percentage (left) and MFI (right) of Jagged1⁺ cells in CD19⁺/CD5⁺ CLL lymphocytes obtained from paired PB, BM and LN samples. Mean % of CD19⁺/CD5⁺/Jagged1⁺ cells in PB 48.68 ± 3.1 vs 50.13 ± 1.9 in BM vs 57.96 ± 3.9 in LN; mean MFI in PB 490 ± 31.9 vs 503.6 ± 32.8 in BM vs 603.3 ± 53.2 in LN. (e) qRT-PCR analysis of *HES1* (e) and *DTX1* (f) mRNA expression in paired PB, BM and LN samples. Mean $\Delta\Delta CT$ of *HES1* 0.29 ± 0.15 in PB vs 0.20 ± 0.11 in BM vs 0.08 ± 0.03 in LN; mean $\Delta\Delta CT$ of *DTX1* 0.86 ± 0.23 in PB vs 1.15 ± 0.23 in BM vs 2.42 ± 0.62 in LN. (g) Western blot analysis using an antibody against total NOTCH1 on total cell lysates of CLL cells from PB, BM and LN in a representative patient. ERK1/2 was used as internal loading control. Red triangles and squares represent paired CLL cells of two *NOTCH1*-mutated patients.

The NOTCH1 pathway is activated during CLL-NLC cell cross talk NLC, cells of myeloid origin that can be differentiated from PBMC of CLL patients³¹ and that support CLL survival, were exploited to recreate a lymphoid niche *in vitro*.³⁴ NLC expressed high levels of *JAG1* mRNA (Figure 6a). Furthermore, supernatants derived from

NLC cultured for 2 weeks contained levels of soluble Jagged1 comparable to those of the plasma of CLL patients (Figure 6b), likely reflecting accumulation during culture. Jagged1 expression was also confirmed at the protein level by immunocytochemistry (Figures 6c and d). In contrast, CLL lymphocytes displayed

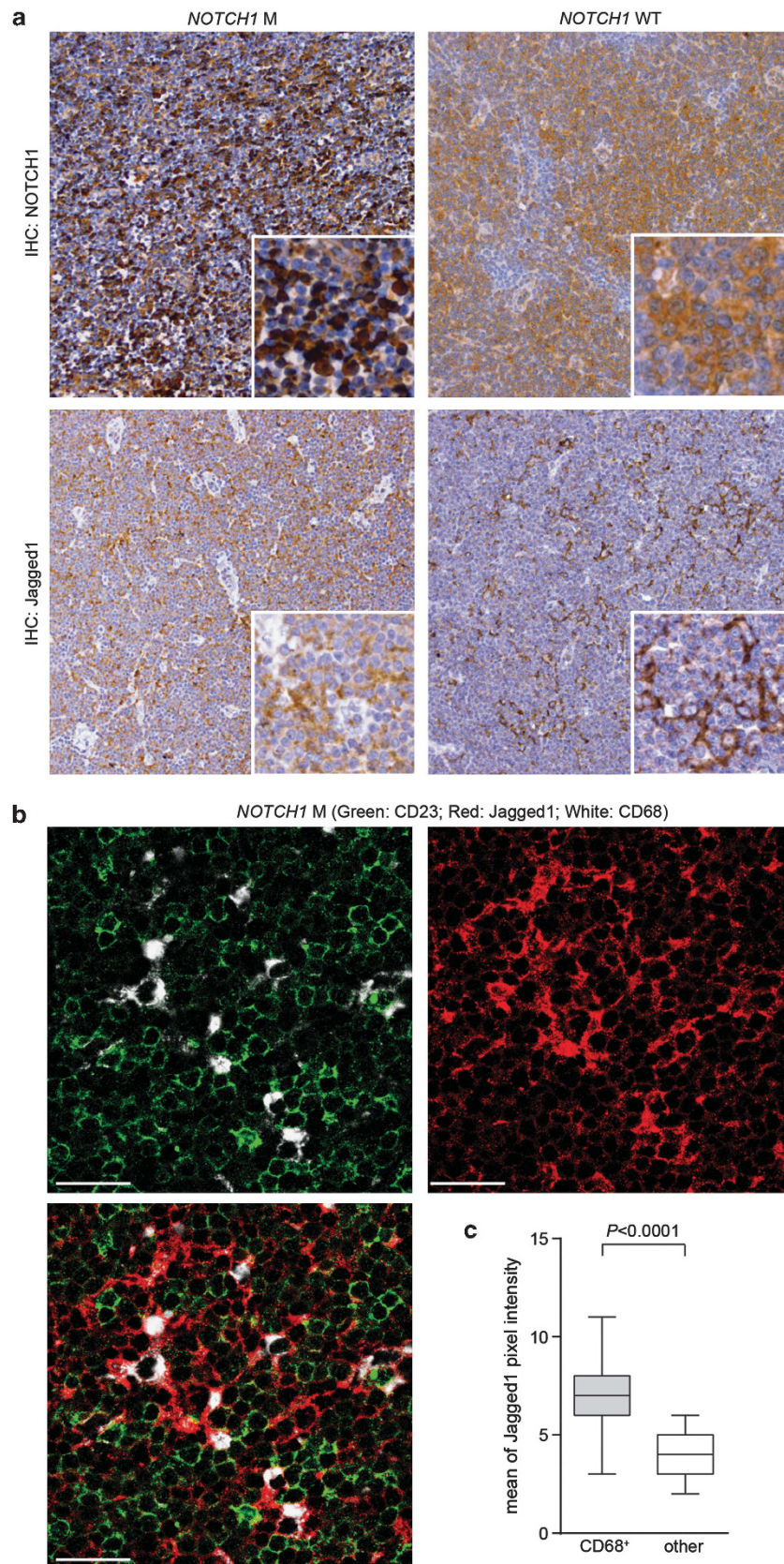


Figure 5. Expression of NOTCH1 and Jagged1 in the CLL LN. **(a)** Anti-total NOTCH1 and anti-Jagged1 immunostaining of representative LN sections from *NOTCH1*-mutated or WT CLL patients. An anti-rabbit HRP-conjugated secondary antibody and 3,3'-diaminobenzidine (brown signal) were used to detect the binding. The inset shows high magnifications of the same sections. Original magnifications are $\times 20$ and $\times 40$. **(b)** Triple staining of a representative LN section from a *NOTCH1*-mutated patient with anti-CD23 (green), -Jagged1 (red) and -CD68 (white). Original magnification is $\times 63$, zoom factor of 2. Scale bars represent 50 μm . **(c)** Quantification of Jagged1 pixel intensity in proximity of CD68⁺ vs CD68⁻ areas. HRP, horse radish peroxidase.

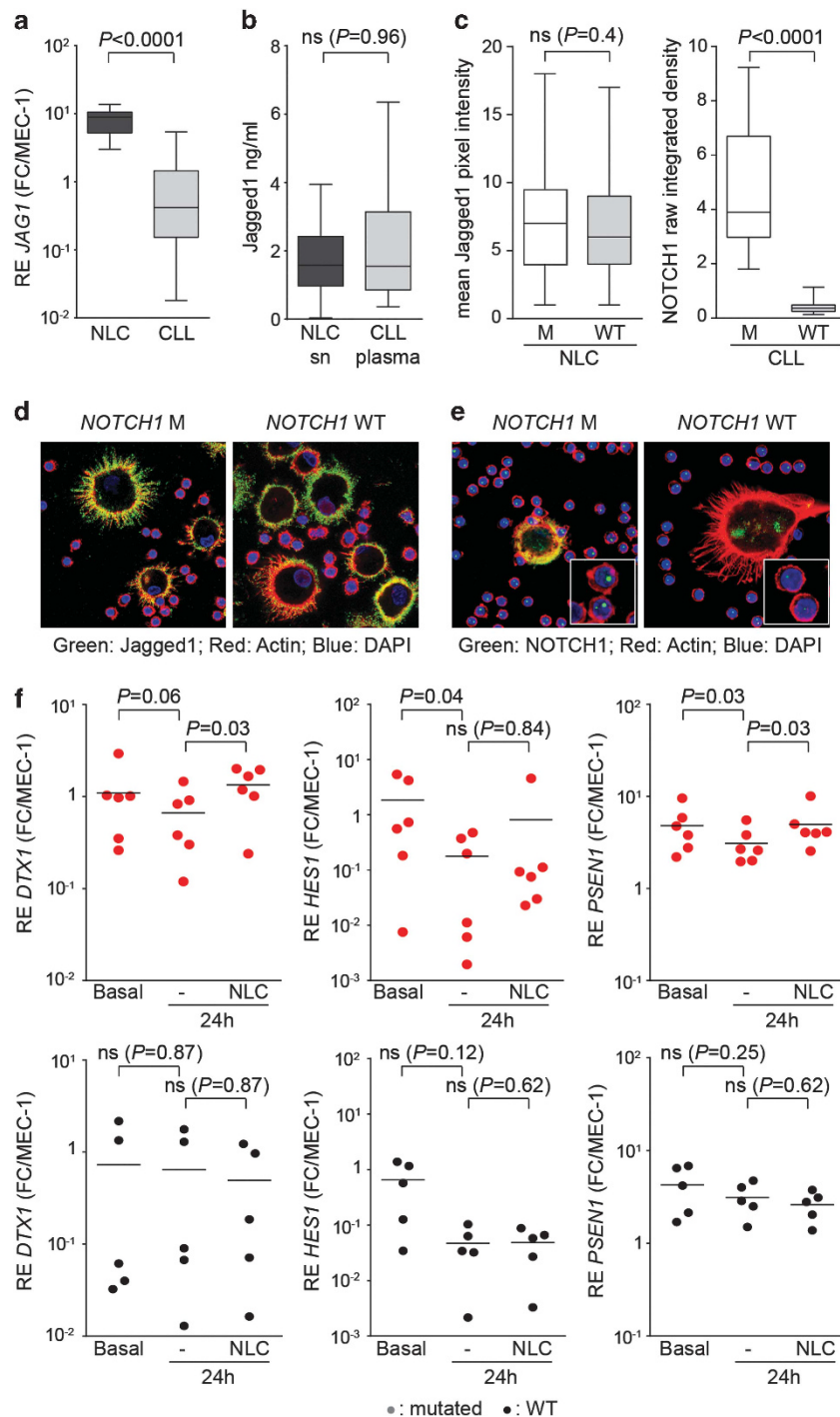


Figure 6. Modulation of the NOTCH1 pathway in CLL/NLC co-cultures. **(a)** qRT-PCR data showing relative expression of *JAG1* mRNA in NLC obtained from eight CLL patients (two *NOTCH1*-mutated and six WT). Levels were compared with those of CLL cells at baseline ($n = 40$). Mean $\Delta\Delta CT$ of *JAG1* 8.35 ± 1.2 in NLC vs 1.06 ± 0.2 in CLL cells. **(b)** Box plots showing the results of an enzyme-linked immunosorbent assay performed on supernatants obtained after culturing PBMC from 17 CLL patients for 14 days. Jagged1 levels in the plasma of the same 17 individuals is shown for comparison. Mean ng/ml in NLC supernatants 1.77 ± 0.23 vs 2.17 ± 0.45 in CLL plasma. **(c)** Quantification of immunofluorescence data presented in **d** and **e**. Immunofluorescence stainings showing expression of Jagged1 (**d**) or NOTCH1 (**e**) on 14 day cultures of PBMC from *NOTCH1*-mutated or -WT CLL patients NLC. Cells were counterstained with phalloidin (red) and DAPI (blue). Original magnification is $\times 63$, zoom factor of 2. Insets represent cropped and zoomed area of the same samples. **(f)** Purified CLL lymphocytes from *NOTCH1*-mutated (red dots, upper part) or -WT (black dots, lower part) CLL patients were cultured (48 h) alone or on NLC layers obtained after 14 day cultures of autologous PBMC before. qRT-PCR analyses were performed to compare expression levels of *DTX1*, *PSEN1* and *HES1*. Mutated patients: mean levels of *DTX1* in basal conditions 1.09 ± 0.39 vs 0.67 ± 0.2 after 48 h vs 1.34 ± 0.26 after 48 h cultures with NLC; mean levels of *HES1* in basal conditions 1.84 ± 0.95 vs 0.18 ± 0.1 after 48 h vs 0.8 ± 0.75 after 48 h cultures with NLC; mean levels of *PSEN1* in basal conditions 4.82 ± 1.09 vs 3.09 ± 0.56 after 48 h vs 4.96 ± 1.07 after 48 h cultures with NLC. WT patients: mean levels of *DTX1* in basal conditions 0.57 ± 0.53 vs 0.48 ± 0.43 after 48 h vs 0.37 ± 0.28 after 48 h cultures with NLC; mean levels of *HES1* in basal conditions 0.52 ± 0.3 vs 0.05 ± 0.02 after 48 h vs 0.04 ± 0.02 after 48 h cultures with NLC; mean levels of *PSEN1* in basal conditions 4.79 ± 1.18 vs 3.52 ± 0.51 after 48 h vs 2.9 ± 0.36 after 48 h cultures with NLC. Relative expression is the result of normalization of CLL values over those of MEC-1, added for calibration purposes.

heterogeneous levels of *JAG1* mRNA (Figure 6a) and low reactivity in immunocytochemistry (Figure 6c), confirming immunofluorescence data (Supplementary Figure 1).

CLL lymphocytes that were still viable and in direct contact with NLC after 2-week cultures were characterized by nuclear localization of NOTCH1, detected using an antibody directed against total NOTCH1 (Figures 6c–e) and suggesting the presence of an active pathway. Fluorescence intensity indicated that *NOTCH1*-mutated cells stained more intensely positive than WT cells ($P < 0.0001$, $n = 4$ for both subgroups, Figures 6c–e).

In a different experiment, purified autologous CLL cells were thawed and plated on differentiated NLC for 48 h before assessing NOTCH1 pathway status. Under these conditions, *DTX1* expression levels were fully rescued ($P = 0.03$, compared with the same cells cultured without NLC, Figure 6f), whereas *HES1* levels decreased after *in vitro* culture and were not significantly modified after the addition of NLC (Figure 6f). *PSEN1* mRNA levels followed the same pattern of *DTX1*, with a decrease in purified cultures and a rescue in NLC cultures ($P = 0.03$, Figure 6f). These effects were evident selectively in the *NOTCH1*-mutated subset as WT samples did not show significant modifications in the expression levels of the genes under analysis. These results indicate that NLC selectively activate the non-canonical pathway in *NOTCH1*-mutated CLL cells.

NOTCH1-mutated CLL cells show partial chemoresistance *in vitro*

Finally, the role of *NOTCH1* mutations in promoting CLL survival and in rescuing leukemic cells from drug-induced apoptosis was studied by *in vitro* assays. When cultured in the presence of fludarabine for 48–72 h, no differences were observed in the apoptotic levels between *NOTCH1*-mutated and WT cases. A subgroup of patients with 17p deletion (del17p) was used as a control and confirmed as chemoresistant (Figure 7a). This observation may be explained by considering that the NOTCH1 pathway is fully inactivated after a few hours in culture. The experiment was then repeated by treating CLL cells with fludarabine in the presence of autologous NLC. In these conditions, *NOTCH1*-mutated patients became markedly resistant to apoptosis ($P = 0.008$ compared with the same cells cultured without NLC, $P = 0.01$ compared with WT samples). Responses of *NOTCH1*-WT and of del17p samples were unaffected by NLC exposure (Figure 7b).

Involvement of the NOTCH1 pathway in mediating resistance to apoptosis was demonstrated using GSilX, which prevents the formation of NICD, even in the presence of the ligand (Figure 2c). Addition of GSilX to CLL cells cultured alone (not shown) or in presence of fludarabine (Figure 7c) did not modify apoptosis, independently of the underlying genetic lesion. However, GSilX pretreatment of CLL cells on a NLC layer reverted the resistant phenotype of the *NOTCH1*-mutated subset (Figure 7d).

The conclusions of the last part of the work indicate that CLL cells from patients harboring *NOTCH1* mutations show a marked resistance to drug-induced apoptosis, which is completely abrogated in the presence NOTCH1 inhibitors.

DISCUSSION

Recent advances in DNA sequencing technology have facilitated analysis of entire genomes of individual cancers and have led to the identification of novel genetic alterations.^{35,36} The ongoing challenge is to make biological sense of the wealth of genetic data by understanding its impact on tumor transformation and progression.³⁷ The ultimate goal is to determine how mutations impact on cancer epidemiology, biology, prognosis and response to therapy.

Applied to CLL, next-generation sequencing studies have shown that at diagnosis, the number of mutations that alter the protein sequence per case is 10–12 on average.^{9,10,38} Among these, *NOTCH1*

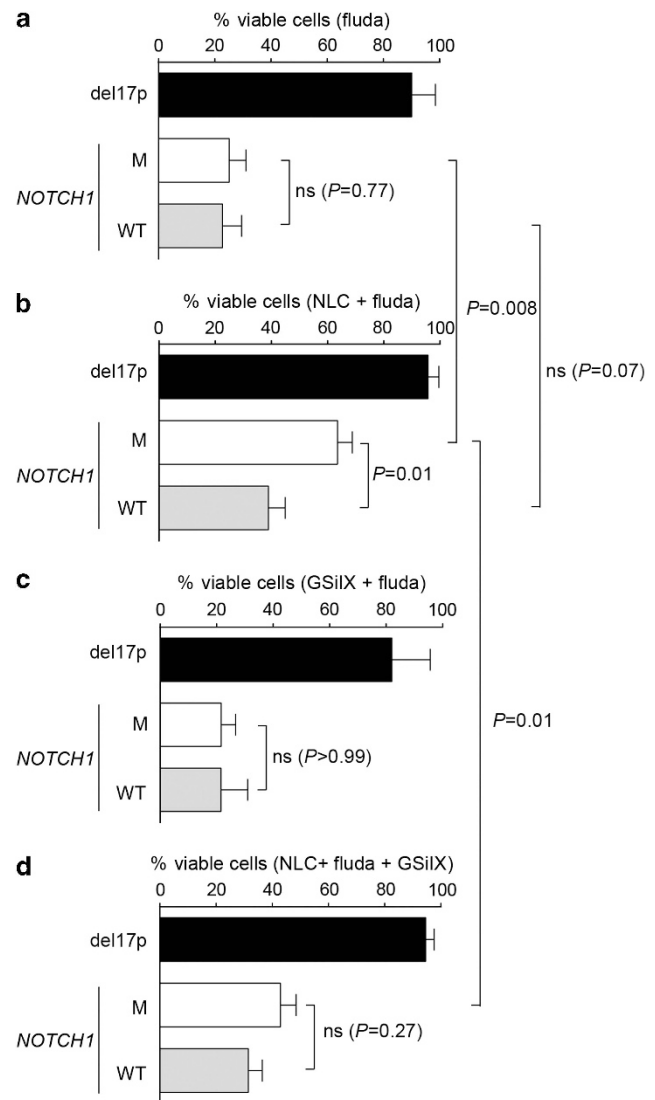


Figure 7. Activation of the NOTCH1 pathway and drug resistance *in vitro*. **(a)** Bar graph showing % of viable cells in del17, *NOTCH1*-mutated or -WT CLL patients cultured in the presence of fludarabine (10 μM for 48 h). Mean % of live cells at 48 h 90.1 ± 8.4 in the del17p vs 25.09 ± 5.9 in the *NOTCH1*-mutated vs 22.7 ± 6.8 in the WT subsets. **(b)** The same experiment was performed after plating purified CLL cells on autologous NLC differentiated from PBMC. Graph shows % of viable cells upon culture in the presence of fludarabine (10 μM for 48 h). Mean % viable cells 95.7 ± 3.8 in the del17p vs 63.5 ± 5.2 in the *NOTCH1*-mutated vs 38.9 ± 5.9 in the WT subsets. **(c)** Bar graph showing the effects of the combination of fludarabine with GSilX on purified CLL cells from del17, *NOTCH1*-mutated or -WT CLL patients. Cells were pretreated with GSilX (5 μM for 20 h) before starting fludarabine incubation (10 μM for 48 h). GSilX was re-added once after 24 h. Mean % of viable cells in del17p 82 ± 13.5 vs 21.6 ± 5.1 in the *NOTCH1*-mutated vs 21.5 ± 9.4 in the WT subset. **(d)** The same experiment described in **c** was performed by culturing purified CLL cells on autologous NLC. Cells were pretreated with GSilX (5 μM for 20 h) before starting fludarabine incubation (10 μM for 48 h). GSilX was re-added once after 24 h of fludarabine culture. Mean % of viable cells in del17p 94.6 ± 3 vs 42.9 ± 5.6 in the *NOTCH1*-mutated vs 31.5 ± 4.9 in the WT subset.

mutations represent one of the most frequent somatic aberrations, affecting 10–15% of patients and conferring an adverse prognosis.^{8,13,39} The present study was undertaken to investigate the expression and functional impact of *NOTCH1* mutations in CLL.

From the results obtained, two main conclusions can be drawn. The first is that *NOTCH1* mutations truncating the PEST domain have a stabilizing effect on the NOTCH1 signaling pathway. Gene expression data show that both the canonical and non-canonical pathways are constitutively upregulated in *NOTCH1*-mutated patients, notwithstanding comparable levels of expression of the receptor and of presenilin1/2, the catalytic subunits of the enzyme that controls NOTCH1 final activation (Supplementary Figure 3). Furthermore, biochemical data indicate selective overexpression of the NICD fragment encoded by the mutant *NOTCH1* allele. This finding is in keeping with the notion that PEST domain mutations impair ubiquitination and degradation of the receptor and are in line with observations obtained in acute lymphoblastic leukemias.⁴⁰ The molecular species produced by the WT allele of *NOTCH1*-mutated patients are also markedly different from those of WT patients, with accumulation of NEXT, the molecular intermediate immediately upstream of NICD, suggesting the presence of compensatory mechanisms to inhibit NOTCH1 activation.

The second conclusion of this work is that the NOTCH1 pathway needs to be activated through micro-environmental connections both in *NOTCH1*-mutated and WT patients. Even if CLL cells express Jagged1 and Jagged2, it appears that CLL–CLL cell interactions are ineffective in activating signaling. This is inferred by the drastic drop in pathway activation when purified CLL cells are kept in culture, an event also occurring in *NOTCH1*-mutated samples. A possible explanation is that these ligands are expressed by CLL cells at a surface density that does not reach the necessary activation threshold or signal intensity.⁴¹ Downregulation of NICD may be attributed to the loss of gamma-secretase activity, apparent at the transcriptional level, underlying a bidirectional control between NICD and presenilin1, already highlighted in other models.⁴² The lack of ligand and the decrease in gamma-secretase activity prevents NICD generation, at the same time inducing relative accumulation of NOTCH1 species upstream of the NICD, clearly visible in western blot assays.

On the other hand, *in vivo* and *in vitro* evidence favors the view that interactions with myeloid cells are critical in activating the NOTCH1 pathway. The analysis of paired samples deriving from different disease compartments indicates that NOTCH1 mRNA and protein expression levels are highest within LN. In this environment, the non-canonical NOTCH1 pathway appears clearly enhanced. Moreover, *NOTCH1*-mutated patients show immunohistochemical evidence of nuclear localization of NOTCH1, as opposed to the cytoplasmic reactivity observed in the WT subset, in line with recent findings.⁴³ In the LN, the Jagged1 ligand is highly expressed by differentiated myeloid elements, suggesting that it is this interaction that activates NOTCH1. Confirmation was obtained by recreating a lymphoid niche *in vitro*, based on co-culture of purified CLL cells and autologous NLC differentiated from PBMC. These experiments allow us to conclude that the non-canonical NOTCH1 pathway is selectively kept active when CLL cells are cultured on an NLC layer. The dissociation between the canonical and non-canonical pathways observed under these conditions and *in vivo* in CLL cells obtained from the LN of paired samples is of interest, particularly in light of recent reports that indicate that *Deltex1* is a major downstream modulator of the NOTCH1 signaling pathway by interfering with the binding of the coactivator p300 to the transcription factor E2A.⁴⁴ This mechanism is relevant in controlling thymocyte maturation.^{26,45}

A final consideration of this work is that activation of NOTCH1 signaling in the LN may contribute to create conditions favoring drug resistance, in line with observations obtained using multiple myeloma models.⁴⁶ The finding that resistance can be overcome through the use of GSis to stop NOTCH1 signaling suggests that the receptor could be a putative therapeutic target, at least in the *NOTCH1*-mutated subset. However, the clinical association

between *NOTCH1* mutations and a chemoresistant phenotype in CLL is highly controversial at this point and requires further elucidation.^{39,47–50} Future studies are needed to evaluate the therapeutic impact of targeting NOTCH1 through the use of GSis or monoclonal antibodies, building on experience gathered in acute lymphoblastic leukemia.^{51–53}

CONFLICT OF INTEREST

The authors declare no conflict of interest.

ACKNOWLEDGEMENTS

Work supported by grants from the Italian Ministries of Education, University and Research (Futuro in Ricerca 2008 no. RBF08ATLH and 2012 no. RBF08ATLH), Italian Ministry of Health (Bando Giovani Ricercatori 2008 no. GR-2008-1138053 and 2010 no. GR-2010-2317594), Associazione Italiana per la Ricerca sul Cancro Foundation (IG 12754, Special Program Molecular Clinical Oncology 5 × 1000 No. 10007 and My First AIRC grant no. 13470), Compagnia di San Paolo (grant no. PMN_call_2012_0071), Fondazione Cariplo (call 2012) and local funds of the University of Turin. FA is supported by a Fondazione Veronesi fellowship. BG is supported by grant from the Croatian Ministry of Science, Education and Sport (no.198-1980955-0953). We would like to thank Katuscia Gizzi and Maria Lamusta for their excellent technical assistance.

AUTHOR CONTRIBUTIONS

FA, BG, SS, TV and CC acquired data; DR, MC, LL GD'A and OJ provided patient samples; GI provided LN samples; FA, DR, GG and GI contributed to interpreting results; FA and SD conceived and designed the work and interpreted results; and SD wrote the paper.

REFERENCES

- Chiorazzi N, Rai KR, Ferrarini M. Chronic lymphocytic leukemia. *N Engl J Med* 2005; **352**: 804–815.
- Zenz T, Mertens D, Kuppers R, Dohner H, Stilgenbauer S. From pathogenesis to treatment of chronic lymphocytic leukaemia. *Nat Rev Cancer* 2010; **10**: 37–50.
- Damle RN, Wasil T, Fais F, Ghiotto F, Valetto A, Allen SL *et al*. Ig V gene mutation status and CD38 expression as novel prognostic indicators in chronic lymphocytic leukemia. *Blood* 1999; **94**: 1840–1847.
- Malavasi F, Deaglio S, Damle R, Cutrona G, Ferrarini M, Chiorazzi N. CD38 and chronic lymphocytic leukemia: a decade later. *Blood* 2011; **118**: 3470–3478.
- Zucchetto A, Bomben R, Dal Bo M, Bulian P, Benedetti D, Nanni P *et al*. CD49d in B-cell chronic lymphocytic leukemia: correlated expression with CD38 and prognostic relevance. *Leukemia* 2006; **20**: 523–525 (author reply 528–529).
- Crespo M, Bosch F, Villamor N, Bellosillo B, Colomer D, Rozman M *et al*. ZAP-70 expression as a surrogate for immunoglobulin-variable-region mutations in chronic lymphocytic leukemia. *N Engl J Med* 2003; **348**: 1764–1775.
- Dohner H, Stilgenbauer S, Benner A, Leupolt E, Krober A, Bullinger L *et al*. Genomic aberrations and survival in chronic lymphocytic leukemia. *N Engl J Med* 2000; **343**: 1910–1916.
- Puente XS, Pinyol M, Quesada V, Conde L, Ordóñez GR, Villamor N *et al*. Whole-genome sequencing identifies recurrent mutations in chronic lymphocytic leukaemia. *Nature* 2011; **475**: 101–105.
- Wang L, Lawrence MS, Wan Y, Stojanov P, Sougnez C, Stevenson K *et al*. SF3B1 and other novel cancer genes in chronic lymphocytic leukemia. *N Engl J Med* 2011; **365**: 2497–2506.
- Gaidano G, Foa R, Dalla-Favera R. Molecular pathogenesis of chronic lymphocytic leukemia. *J Clin Invest* 2012; **122**: 3432–3438.
- Knight SJ, Yau C, Clifford R, Timbs AT, Sadighi Akha E, Dreau HM *et al*. Quantification of subclonal distributions of recurrent genomic aberrations in paired pre-treatment and relapse samples from patients with B-cell chronic lymphocytic leukemia. *Leukemia* 2012; **26**: 1564–1575.
- Landau DA, Carter SL, Stojanov P, McKenna A, Stevenson K, Lawrence MS *et al*. Evolution and impact of subclonal mutations in chronic lymphocytic leukemia. *Cell* 2013; **152**: 714–726.
- Fabbri G, Rasi S, Rossi D, Trifonov V, Khatibian H, Ma J *et al*. Analysis of the chronic lymphocytic leukemia coding genome: role of NOTCH1 mutational activation. *J Exp Med* 2011; **208**: 1389–1401.
- Balatti V, Bottoni A, Palamarchuk A, Alder H, Rassenti LZ, Kipps TJ *et al*. NOTCH1 mutations in CLL associated with trisomy 12. *Blood* 2012; **119**: 329–331.
- Del Giudice I, Rossi D, Chiaretti S, Marinelli M, Tivolari S, Gabrielli S *et al*. NOTCH1 mutations in +12 chronic lymphocytic leukemia (CLL) confer an unfavorable

- prognosis, induce a distinctive transcriptional profiling and refine the intermediate prognosis of +12 CLL. *Haematologica* 2012; **97**: 437–441.
- 16 Yuan JS, Kousis PC, Suliman S, Visan I, Guidos CJ. Functions of notch signaling in the immune system: consensus and controversies. *Annu Rev Immunol* 2010; **28**: 343–365.
 - 17 Lobry C, Oh P, Aifantis I. Oncogenic and tumor suppressor functions of Notch in cancer: it's NOTCH what you think. *J Exp Med* 2011; **208**: 1931–1935.
 - 18 Jarriault S, Brou C, Logeat F, Schroeter EH, Kopan R, Israel A. Signalling downstream of activated mammalian Notch. *Nature* 1995; **377**: 355–358.
 - 19 Kato H, Taniguchi Y, Kurooka H, Minoguchi S, Sakai T, Nomura-Okazaki S et al. Involvement of RBP-J in biological functions of mouse Notch1 and its derivatives. *Development* 1997; **124**: 4133–4141.
 - 20 Castel D, Mourikis P, Bartels SJ, Brinkman AB, Tajbakhsh S, Stunnenberg HG. Dynamic binding of RBPJ is determined by Notch signaling status. *Genes Dev* 2013; **27**: 1059–1071.
 - 21 Davis RL, Turner DL. Vertebrate hairy and enhancer of split related proteins: transcriptional repressors regulating cellular differentiation and embryonic patterning. *Oncogene* 2001; **20**: 8342–8357.
 - 22 Iso T, Kedes L, Hamamori Y. HES and HERP families: multiple effectors of the Notch signaling pathway. *J Cell Physiol* 2003; **194**: 237–255.
 - 23 Matsuno K, Eastman D, Mitsiades T, Quinn AM, Carcanci ML, Ordentlich P et al. Human Deltex is a conserved regulator of Notch signalling. *Nat Genet* 1998; **19**: 74–78.
 - 24 Kopan R, Ilagan MX. The canonical Notch signaling pathway: unfolding the activation mechanism. *Cell* 2009; **137**: 216–233.
 - 25 Ordentlich P, Lin A, Shen CP, Blaumueller C, Matsuno K, Artavanis-Tsakonas S et al. Notch inhibition of E47 supports the existence of a novel signaling pathway. *Mol Cell Biol* 1998; **18**: 2230–2239.
 - 26 Jang J, Choi YI, Choi J, Lee KY, Chung H, Jeon SH et al. Notch1 confers thymocytes a resistance to GC-induced apoptosis through Deltex1 by blocking the recruitment of p300 to the SRG3 promoter. *Cell Death Differ* 2006; **13**: 1495–1505.
 - 27 Huber RM, Rajski M, Sivasankaran B, Moncayo G, Hemmings BA, Merlo A. Deltex-1 activates mitotic signaling and proliferation and increases the clonogenic and invasive potential of U373 and LN18 glioblastoma cells and correlates with patient survival. *PLoS One* 2013; **8**: e57793.
 - 28 Rosati E, Sabatini R, Rampino G, Tabilio A, Di Ianni M, Fettucciari K et al. Constitutively activated Notch signaling is involved in survival and apoptosis resistance of B-CLL cells. *Blood* 2009; **113**: 856–865.
 - 29 Hajdu M, Sebestyen A, Barna G, Reiniger L, Janosi J, Sreter L et al. Activity of the notch-signalling pathway in circulating human chronic lymphocytic leukaemia cells. *Scand J Immunol* 2007; **65**: 271–275.
 - 30 Paganin M, Ferrando A. Molecular pathogenesis and targeted therapies for NOTCH1-induced T-cell acute lymphoblastic leukemia. *Blood Rev* 2011; **25**: 83–90.
 - 31 Burger JA, Tsukada N, Burger M, Zvaifler NJ, Dell'Aquila M, Kipps TJ. Blood-derived nurse-like cells protect chronic lymphocytic leukemia B cells from spontaneous apoptosis through stromal cell-derived factor-1. *Blood* 2000; **96**: 2655–2663.
 - 32 Deaglio S, Vaisitti T, Aydin S, Bergui L, D'Arena G, Bonello L et al. CD38 and ZAP-70 are functionally linked and mark CLL cells with high migratory potential. *Blood* 2007; **110**: 4012–4021.
 - 33 Brou C, Logeat F, Gupta N, Bessia C, LeBail O, Doedens JR et al. A novel proteolytic cleavage involved in Notch signaling: the role of the disintegrin-metalloprotease TACE. *Mol Cell* 2000; **5**: 207–216.
 - 34 Deaglio S, Vaisitti T, Bergui L, Bonello L, Horenstein AL, Tamagnone L et al. CD38 and CD100 lead a network of surface receptors relaying positive signals for B-CLL growth and survival. *Blood* 2005; **105**: 3042–3050.
 - 35 Meyerson M, Gabriel S, Getz G. Advances in understanding cancer genomes through second-generation sequencing. *Nat Rev Genet* 2010; **11**: 685–696.
 - 36 Mardis ER. A decade's perspective on DNA sequencing technology. *Nature* 2011; **470**: 198–203.
 - 37 Chin L, Hahn WC, Getz G, Meyerson M. Making sense of cancer genomic data. *Genes Dev* 2011; **25**: 534–555.
 - 38 Landau DA, Wu CJ. Chronic lymphocytic leukemia: molecular heterogeneity revealed by high-throughput genomics. *Genome Med* 2013; **5**: 47.
 - 39 Rossi D, Rasi S, Fabbri G, Spina V, Fangazio M, Forconi F et al. Mutations of NOTCH1 are an independent predictor of survival in chronic lymphocytic leukemia. *Blood* 2012; **119**: 521–529.
 - 40 Weng AP, Ferrando AA, Lee W, Morris JPt, Silverman LB, Sanchez-Irizarry C et al. Activating mutations of NOTCH1 in human T cell acute lymphoblastic leukemia. *Science* 2004; **306**: 269–271.
 - 41 Van de Walle I, De Smet G, De Smedt M, Vandekerckhove B, Leclercq G, Plum J et al. An early decrease in Notch activation is required for human TCR-alpha-beta lineage differentiation at the expense of TCR-gammadelta T cells. *Blood* 2009; **113**: 2988–2998.
 - 42 Lleo A, Berezovska O, Ramdya P, Fukumoto H, Raju S, Shah T et al. Notch1 competes with the amyloid precursor protein for gamma-secretase and down-regulates presenilin-1 gene expression. *J Biol Chem* 2003; **278**: 47370–47375.
 - 43 Kluk MJ, Ashworth T, Wang H, Knoechel B, Mason EF, Morgan EA et al. Gauging NOTCH1 activation in cancer using immunohistochemistry. *PLoS One* 2013; **8**: e67306.
 - 44 Yamamoto N, Yamamoto S, Inagaki F, Kawaichi M, Fukamizu A, Kishi N et al. Role of Deltex-1 as a transcriptional regulator downstream of the Notch receptor. *J Biol Chem* 2001; **276**: 45031–45040.
 - 45 Deftos ML, Huang E, Ojala EW, Forbush KA, Bevan MJ. Notch1 signaling promotes the maturation of CD4 and CD8 SP thymocytes. *Immunity* 2000; **13**: 73–84.
 - 46 Nefedova Y, Cheng P, Alsina M, Dalton WS, Gabrilovich DI. Involvement of Notch-1 signaling in bone marrow stroma-mediated *de novo* drug resistance of myeloma and other malignant lymphoid cell lines. *Blood* 2004; **103**: 3503–3510.
 - 47 Villamor N, Conde L, Martinez-Trillos A, Cazorla M, Navarro A, Bea S et al. NOTCH1 mutations identify a genetic subgroup of chronic lymphocytic leukemia patients with high risk of transformation and poor outcome. *Leukemia* 2013; **27**: 1100–1106.
 - 48 Foa R, Del Giudice I, Guarini A, Rossi D, Gaidano G. Clinical implications of the molecular genetics of chronic lymphocytic leukemia. *Haematologica* 2013; **98**: 675–685.
 - 49 Oscier DG, Rose-Zerilli MJ, Winkelmann N, Gonzalez de Castro D, Gomez B, Forster J et al. The clinical significance of NOTCH1 and SF3B1 mutations in the UK LRF CLL4 trial. *Blood* 2013; **121**: 468–475.
 - 50 Stilgenbauer S, Busch R, Schnaiter A, Paschka P, Rossi M, Döhner K et al. Gene mutations and treatment outcome in chronic lymphocytic leukemia: results from the CLL8 trial. *Blood* 2012; **120**: 433.
 - 51 Tosello V, Ferrando AA. The NOTCH signaling pathway: role in the pathogenesis of T-cell acute lymphoblastic leukemia and implication for therapy. *Ther Adv Hematol* 2013; **4**: 199–210.
 - 52 Ma W, Gutierrez A, Goff DJ, Geron I, Sadarangani A, Jamieson CA et al. NOTCH1 signaling promotes human T-cell acute lymphoblastic leukemia initiating cell regeneration in supportive niches. *PLoS One* 2012; **7**: e39725.
 - 53 Agnusdei V, Minuzzo S, Frasson C, Grassi A, Axelrod F, Satyal S et al. Therapeutic antibody targeting of Notch1 in T-acute lymphoblastic leukemia xenografts. *Leukemia* 2014; **28**: 278–288.

Supplementary Information accompanies this paper on the Leukemia website (<http://www.nature.com/leu>)